Numerical and Experimental Investigation of the Aerodynamic Performances of Counter-Rotating Rotors

Ibrahim Beldjilali, Adel Ghenaiet

Abstract—The contra-rotating axial machine is a promising solution for several applications, where high pressure and efficiencies are needed. Also, they allow reducing the speed of rotation, the radial spacing and a better flexibility of use. However, this requires a better understanding of their operation, including the influence of second rotor on the overall aerodynamic performances. This work consisted of both experimental and numerical studies to characterize this counter-rotating fan, especially the analysis of the effects of the blades stagger angle and the inter-distance between the rotors. The experimental study served to validate the computational fluid dynamics model (CFD) used in the simulations. The numerical study permitted to cover a wider range of parameter and deeper investigation on flow structures details, including the effects of blade stagger angle and inter-distance, associated with the interaction between the rotors. As a result, there is a clear improvement in aerodynamic performance compared with a conventional machine.

Keywords—Aerodynamic performance, axial fan, counter rotating rotors, CFD, experimental study.

I. Introduction

FANS are unavoidable accessories and also very widely used in many fields and various common applications. The need for better performance and reduced volumes with the slightest noise is a permanent research theme. Fans with two counter-rotating rotors are a promising solution to reduce energy consumption, weight, and volume. Indeed, the addition of a second rotor rotating in the opposite direction of the first rotor reduces the tangential component of the speed, and better homogenizes the flow downstream of the rear rotor, these machines have better energy performance and aeroacoustics.

The problematic in this study is to determine by an experimental approach the overall and resulting performances of the interaction between the two rotors of this counter-rotating fan stage and a complementary numerical study using the ANSYS-CFX CFD software, is intended to provide a detailed description of the nature of the flows, and to predict the aerodynamic characteristics as well as the unstable phenomena associated with its flow. This study made it possible to elaborate the effect of the blade stagger angle and

inter-distances at a nominal operating speed. In the first place for the case of a simple fan, we will study the effect of the blade stagger angle of the rotor. Next, we will focus on the counter-rotating fan, for which we study the effect of the angle of the first rotor and the corresponding angle of the second rotor followed by a study of the effect of the axial inter-distance. The reverse engineering and the realization of the blades of the second counter-rotating rotor (RR) of the test bench are essential during this study as well as the establishment of the means of measurements realized (static and total pressure rise, flow, power ...).

In the experimental part, we will first present the realization method of the second counter-rotating rotor (RR) and the preparation of the test bench with the counter-rotating movement to place the two rotors at a time, then the methodology followed for the digitization and reconstruction of the 3D geometry of the fan blades by a three-dimensional laser measuring machine (Laser MMT). Finally, the choice of boundary conditions and the adopted simulation parameters. For the purpose of validation, comparisons will be made between performances estimated numerically and those measured experimentally. We show the gain achieved by a two-stage counter-rotating configuration. This part is focused on the effects of the stagger angle ξ and the variation of the axial distance *d*. In particular, the effects related to the interaction between the rotors are presented.

II. Bibliographic Review

A. Axial Fans

Fans, unlike compressors, achieve a low pressure rise. This is named a pressure difference ΔP instead of a pressure ratio. They allow higher flow rates compared to centrifugal machines. They are found in various very common applications requiring a ventilation system or they are used to renew the ambient air, etc.

Fig. 1 Simple and counter-rotating fan

Ibrahim Beldjilali is with the Energy Department, Faculty of Mechanical Engineering, University of Sciences and Technology Mohamed Boudiaf , BP 1505, Bir El Djir, 31000 Oran, Algeria (e-mail: beldjilali.brahim@gmail.com).

Adel Ghenaiet is with the Laboratory of Energetic Mechanics and Conversion Systems, Faculty of Mechanical Engineering, University of Sciences and Technology Houari Boumediene, BP32 El-Alia, Bab-Ezzouar, 16111 Algiers, Algeria (e-mail: ag1964@yahoo.com).

B. Axial Counter-Rotating Turbomachines

The stage of a counter-rotating turbomachine is composed of two rotors rotating in opposite directions, the front rotor (FR) and the rear rotor (RR). The role of the rear rotor is double, firstly, it rectifies the flow from the first rotor, in the manner of a diffuser converting the kinetic energy of rotation into static pressure energy. Secondly it contributes by its rotation to add additional energy to the fluid. The presence of the two rotors leads to the introduction of many free parameters for the design, such as the blade loading distribution, the axial distance, the ratio of rotation speeds, blades stagger and the ratio of the diameters [1].

Research on counter-rotating systems applied to turbomachines dates back to the 19th century [2] for boat thrusters. So, in the early 20th century, Lesley [3] performed a series of experiments on counter-rotating thrusters. For these, as we know, the interest is the maximum of thrust. But, in the early 1990s, open counter-rotating rotors were rejected because of high levels of aeroacoustics noise emission, which was one of the main challenges of introducing counter-rotating rotors open in civil aviation. Recently, Shigemitsu et al. [4] turned the interest of research to counter-rotating fans. This research proved that numerical computation could be a convenient way of examining the complex flow field in counter-rotating fans. For axial spacing between front and rear rotor, Shigemitsu et al. [5] studied the influence of distance d on the static pressure field, by experimentation and numerical simulations. This distance had a slight influence on the static pressure rise of the front rotor, but gradually decreased the static pressure of the rotor. He could conclude that there is a limit axial distance, beyond the performances deteriorate.

III. EXPERIMENTAL STUDY

In order to locate the operating range of the single-stage or double-stage counter-rotating fan with different configurations and to check the conformity of the numerical results, it is necessary to carry out experimental tests. This mainly concerns rotational speed measurements, static and total pressure, air flow, power absorbed, and fan compression efficiency.
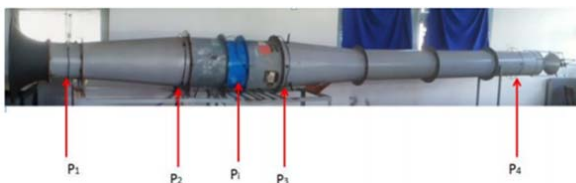

Fig. 2 Test bench realized, p: static pressure

A. Realization of the 2nd Counter-Rotating Rotor

Reverse engineering and the realization of the blades of the second counter-rotating rotor (RR) is essential for this study. To do this, we first have to create a CAD model from a geometry previously obtained from the complete dawn that was realized on the SolidWorks software. Secondly, by the realization of the model to be molded which was realized in

resin by a 3D digital printer. The blades of the 2nd rotor were molded in aluminum and followed by a surface treatment to ensure good robustness and stability to the bench.

Fig. 3 Complete geometry of the counter-rotating rotor made

B. Instrumentations

For the measurement of the air temperature, a digital thermocouple was used.

Fig. 4 Digital thermocouple

A multitube in U filled with distilled water is used, fixed to a table graduated in millimeters, inclined at an angle of 30°.
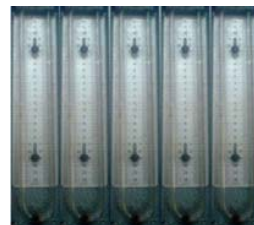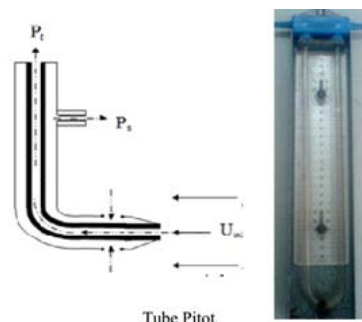

Fig. 5 Multitube

Fig. 6 Pitot tube

For calibration of the flowmeter and obtaining profiles of

the axial velocities, a Pitot tube was used.

$$V = \sqrt{\frac{2 \rho_{eau} \, g \, \Delta h_{eau}}{\rho_{air}}} \qquad (1)$$

The volume flow will be calculated by the following discretized formula:

$$Q_v = 2\pi \sum V_i r_i \Delta r_i \qquad (2)$$

C. Calibration of the Flowmeter

For this purpose, the curve of variation of the flow as a function of the pressure at the neck has been established $\left(Qv = f(\Delta P_1)\right)$ where $\Delta P_1 = (P_a - P_1)$.
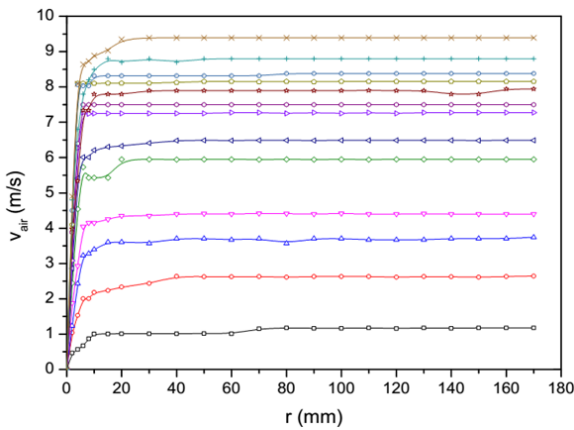

Fig. 7 Velocity as a function of the radius
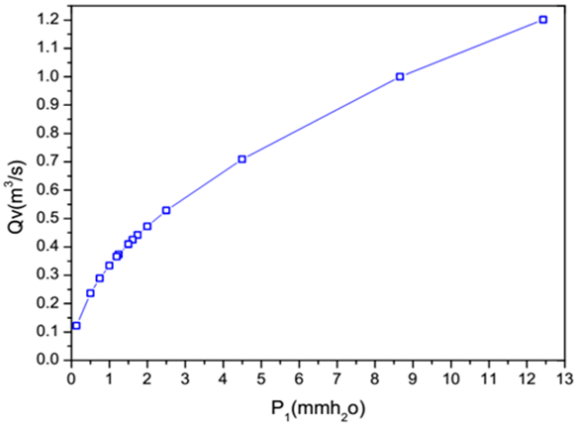
Fig. 8 Flow as a function of the pressure

From this curve, we can approximate the law giving the variation of the volumetric flow rate as a function of the pressure measured at the inlet which is:

$$Qv = 0.1067 \, \Delta P_1^{0.5} \qquad (3)$$

D. Simple Fan Performance

Pressure Elevation and Efficiency

It can be seen that the pressure difference decreases with increasing flow and the slope changes from a certain flow rate towards high flow rates (from 0.6 m³/s), for blade stagger angle of single rotor SR, $\xi_{SR} = 62$ °, it is almost linear for low flow rates. The speeds being high, the static pressures measured will necessarily be low.

For the isentropic total-static efficiency ηt-s, it can be seen that it increases with flow and reaches a maximum of η_{t-s} =51.5% at a flow rate around Qv=1.45 m³/s, for an angle ξ_{SR} = 62 °

As shown in Fig. 5, the maximum flow achieved by the fan is limited to a value equal to 1.45 m³/s. This limitation of flow imposes the choice of the best configuration which must also ensure a better efficiency and also guarantees a great compression ΔP. Therefore, it is clear that the efficiency of the configuration ξ_{SR}=62°, which is nominal, at a flow rate Q = 1.45 m³/s, the greatest pressure rise ΔP_t = 190 Pa.

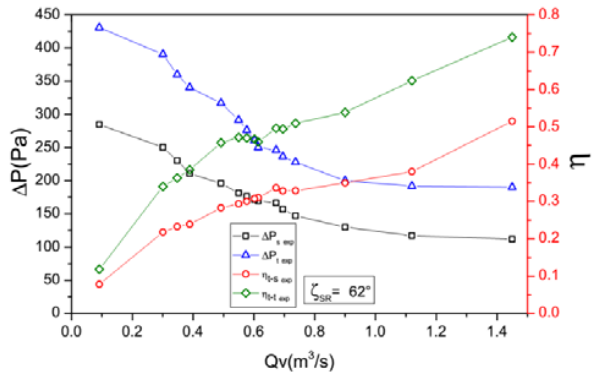

Fig. 9 Pressure elevation and efficiency (ξ_{SR}=62°)

Load Factor

Note that the load factor is inversely proportional to the coefficient of flow and the form is similar to that of the pressure difference. This variation of the load factor which is the parameter which links the increase of the total enthalpy (total pressure) to the peripheral speed and allows to give an idea on the aerodynamic loading. The increase in the flow coefficient implies a decrease in the pressure difference, which induces the reduction of the load factor.
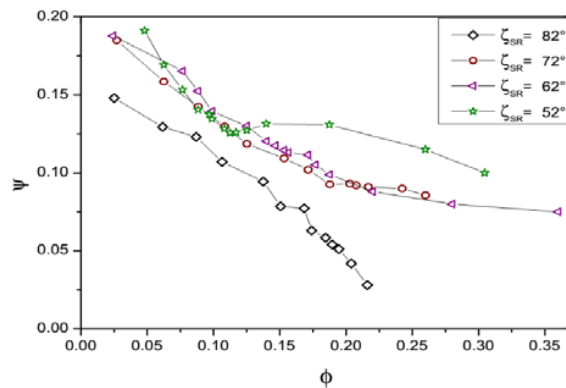

Fig. 10 Load factor as a function of flow coefficient

We have characterized the operation of the simple case and

deduced the performances and the different parameters which characterize it. In addition, the nominal operating point was determined and we can say that the setting (ξ_{SR}=62°) gives more performance in terms of efficiency and pressure increase. ensuring a wider range of flow.

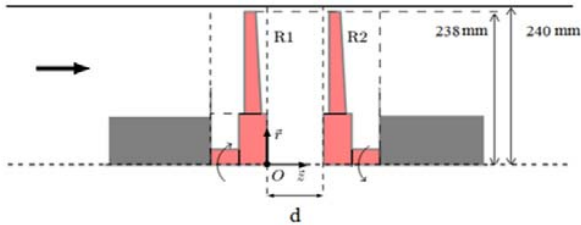### E. Performance of the Counter-Rotating Rotor Fan

Fig. 11 The counter-rotating rotor

Elevation of the Static Pressure

By placing the rear rotor (RR) behind the front rotor (FR), the static pressure rise curves of the counter-rotating stage CR (Fig. 7) indicate a clear improvement, for example, there is a significant increase for the highs rates. For the angle (ξ_{SR}=62°), if we take the flow Qv =1.25 m³/s, ΔPs =324 Pa is an increase of 212 Pa.
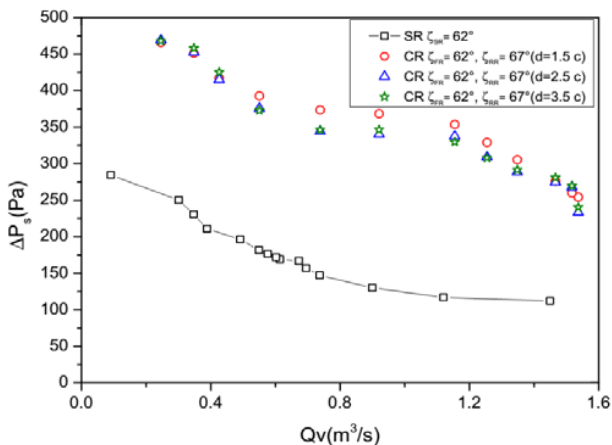

Fig. 12 Static pressure elevation as a function of the flow (ξ_{FR}=62°)

Efficiency

The nominal flow rate of the single fan (ξ_{SR}=62°) is greater than the counter-rotating fan flow (ξ_{SR}=62°) with a maximum total static efficiency of 64 % at a flow rate of Qv_{nom} =1.45 m³/s. Whereas for the counter-rotating fan, the total static efficiency is 71.2 % at a flow rate of Qv = 1.25 m³ / s for a distance of 1.5 from the average cord, an improvement of the total static efficiency of 12% at the nominal flow rate and globally over the entire operating range. In high flow rates, the measured efficiency values are below that of the single fan. This increase in efficiency is not only brought about by an increase in the static pressure rise but also by the reduction in powers consumed by the rotor R2 in the CR configuration, which therefore has a positive effect which tends to reduce the power consumption. In addition, there is a "break" of the slope from Qv = 0.7 m³/s, where the slope becomes even higher for

the counter-rotating rotor configuration. However, static total efficiency curves are above that of a single rotor at any point in the range.

The nominal flow rate of the counter-rotating stage is close to the nominal flow rate of the simple case, but the static pressure rise shows a large difference. The total static efficiency of the counter-rotating system is higher for all configurations, which represents an increase of about 12% for ξ = 62° compared to a rotor R1 alone. The static and total pressure rise characteristic curves and the efficiency have a similar shape to that of the counter-rotating one. This is in agreement with the work of Shigemitsu et al. [6]. However, the single-stage efficiency curve is relatively flat and the difference in efficiency is not significant at low flow rates, this is due to the ability of the counter-rotating system to have a large flow to better identify the operating range.
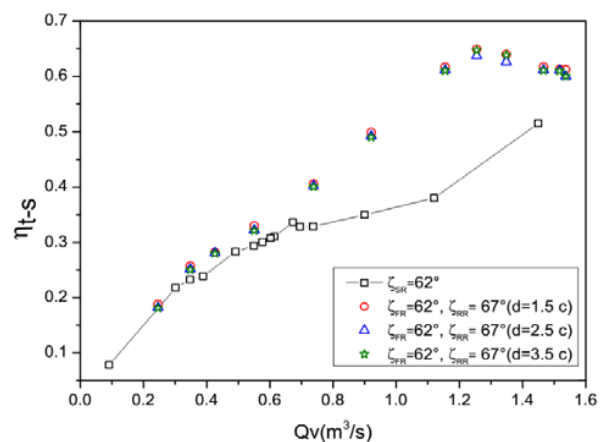

Fig. 13 Total static efficiency as a function of flow ξ_{FR} = 62 °

Effect of the Axial Distance

We note that at a small distance of 1.5 of cord (1.5c) it is beneficial for performance of the stage in all configurations. In addition, for the setting (ξ_{FR} = 62 °) the total static efficiency remains around the value 64.94%. During this evolution of the distance, the static pressure rise decreases moderately (from 324 Pa to d = 1.5 c at 301 Pa at d = 3.5c). Nevertheless, the total static efficiency varies slightly, following a decrease in the total power consumption of the stage, and especially for the RR rotor. Then, when d increases, there is a slight decrease in the static pressure rise which has more influence than the continuous decrease of the total power absorbed. This is why the static total efficiency decreases to 64. 7% at d = 3.5c, caused by the drop in the elevation of the static pressure when d increases. At the input of RR, the axial speed remains practically constant. In addition, the tangential velocity decreases because of friction losses and wake between FR and RR. There is a speed deficit which causes the decrease of the dynamic pressure between FR and RR. It is noted that the distance d has little influence on the flow angle over the entire height of the blade at the exit of the FR. Against, the deflection of the flow is important at the trailing edge of the blade, creating heavy losses. On the other hand, when d

increases, the angle of incidence of RR decreases and this decreases the load and the deflection of the air flow. Finally, two explanations can interpret the static pressure drop for a distance d important. The first cause comes from the FR, when the distance d is important, the deflection angle of the flow at the outlet of FR increases substantially and thus the flow does not follow well the blade. The second cause comes from the decrease of the speed between the FR and RR due to friction and wake, and axial and tangential speed deficit causes the decrease of the dynamic pressure between FR and RR, so there is less work produced by the blade when the axial distance is large.

IV. NUMERIC STUDY

The single fan is divided into three areas. The first domain is an extension that has a shape at the spherical inlet plus a cylinder to the rotor, the second domain is the rotor, the last domain is the profiled cone, which has an ogival shape. The counter-rotating fan is divided into five areas of calculation by adding the rotor2 and the axial inter-distance. The calculation tool used to numerically solve the flow equations is CFX with turbulence model k-ω SST.
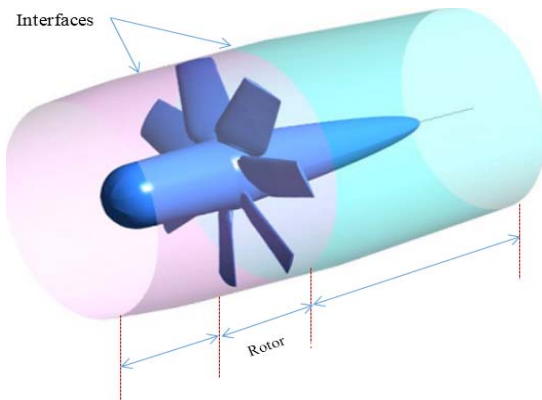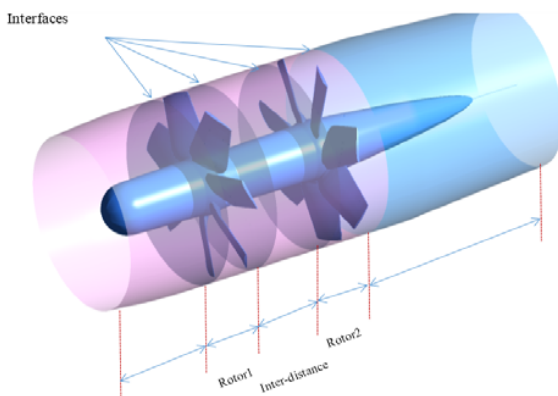

Fig. 14 Domain of calculation of the single fan SR

Fig. 15 Domain of calculation of the counter-rotating fan CR

A. Generation of Meshes

For the mesh of the rotors, we used the *turbogrid (*CFX*).* The meshes obtained are structured type and are based on a decomposition of the domain of computation in blocks relative to each part (hexahedral meshes in H-grid and O-grid for the rotor) completed at their ends by meshes in H. The end clearance close to the walls of the rotor blades is discretized using an O-mesh and a hexahedral mesh for the rest of the domain allowing a correct passage of information between the mesh of the rotor and the mesh of the upstream and downstream part whose radial distribution is much larger. The mesh of the front and rear extensions as well as the inter-distance have been made by means of the software "Gambit", which provides the ability to create meshes with different types according to the geometry
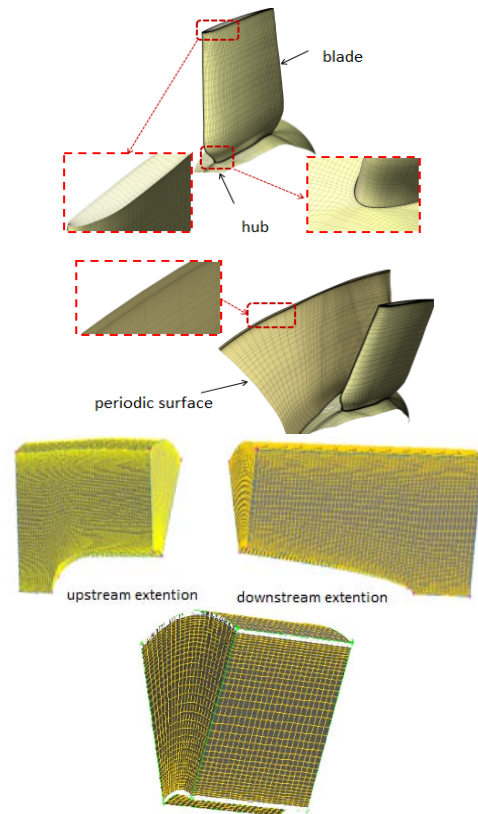

Fig. 16 Mesh of blade, extensions, and inter-distance

B. Aerodynamic Study of the Single Fan

Static Pressure Rise and Efficiency

From a practical point of view, performance curves are shown in terms of static pressure rise versus flow. This makes it possible to know if the fan used is able to overcome the losses. For the value of the nominal flow rate, for the setting (ξ = 62 °) at the flow rate of 1.87 m³/s, ΔPs = 66 Pa at the flow rate of 1.87 m³/s.

Two types of efficiency are studied namely, the total-static efficiency that has been defined to characterize the performance and the diffusion of a bladed fan by allowing to characterize the transfer of kinetic energy in pressure. The total-total efficiency uses a comparison between the real transformation (not-adiabatic and irreversible) and the ideal

isentropic transformation equivalent between the total quantities.

It can be seen from these figures that the increase in Blade Stagger Angle is systematically accompanied by a variation in efficiency, which is explained by the work that receives the fluid through the rotor which is related to the capacity of the rotor to produce on the flow a deviation V_θ, and to create more depression on the extrados and overpressure on the intrados, and therefore, more aerodynamic force.

From these curves, the nominal flow rate is around $Q = 1.87$ m^3/s for the angle ($\xi = 62$ °) with a total-static efficiency of about 64.7%.

Effect of the Blade Stagger Angle

This section focuses on the effect of blade stagger angle parameters on the flow and its impact on the aerodynamic performance of the single fan.

The elevation of the static pressure for the angle ($\xi = 52$ °) is slightly higher than that obtained for ($\xi = 62$ °) at low flow and conversely at high flow and that the static pressure of $\xi = 62$ ° reaches its maximum flow for a lower pressure. Nevertheless, for $\xi = 52$ °, the maximum flow rate obtained is lower than that of ($\xi = 62$ °), this is justified by exceeding the rotor adaptation range which results in a low rise in static pressure and obviously a low efficiency. However, the static pressure elevation curve for blade stagger angle $\xi = 72$ ° is above the curve obtained for $\xi = 82$ ° at any point in the range. The nominal flow rate of $\xi = 82$ ° is lower compared to the case of $\xi = 72$ ° with a maximum efficiency of 53%. At low flow rates, the stall zone is shifted to a higher flow rate by increasing the blade stagger angle, which is justified by the bad incidence of the flow which hastens the aerodynamic stall.
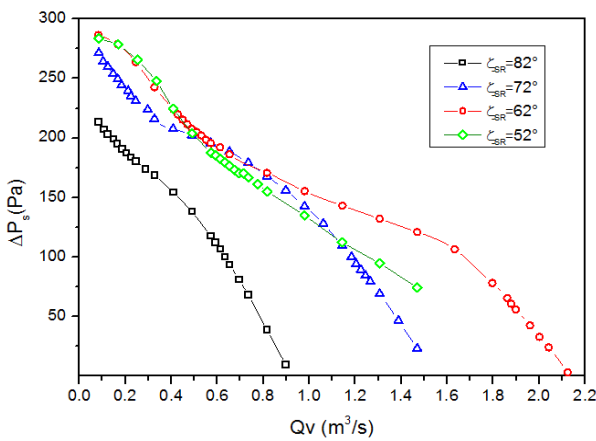

Fig. 17 Static pressure (ξ_{SR} = 82 °, 72 °, 62 °, 52 °)

By recapitulating, it is clear that the best efficiency and elevation of static pressure are predicted for a configuration with an angle $\xi = 62$ °. For $\xi = 72$ °, at the nominal flow rate of 1.18 m^3/s, a static pressure rise of $\Delta P_s = 100$ is measured, with a total-static efficiency of 63% and total-total efficiency of 73%, for $\xi = 62$ °, at the nominal flow rate of 1.87 m^3/s, a static pressure rise $\Delta P_s = 66$ Pa are measured, with a total-

static efficiency of 64.7%. From these values, we can say that the blade stagger angle $\xi = 62$ ° allows to have the best efficiency, this has already been verified as we saw in the experimentation part. This conclusion remains valid from an experimental view, because of the limitation of the operating range imposed by the test bench.
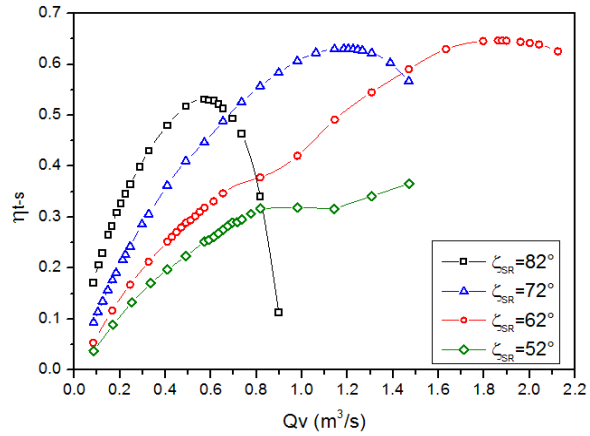

Fig. 18 Static total efficiency (ξ_{SR} = 82 °, 72 °, 62 °, 52 °)

C. Aerodynamic Study of the Counter-Rotating Fan

Static Pressure Elevation and Efficiency

Several configurations will be examined, blade stagger angle $\xi = 62$ ° and axial distances: d=1c, d= 1.5c, d= 2c and d=3c such that c is the medium cord in order to determine the optimal configuration in term of stagger angle and inter-distance which produces the best performances.
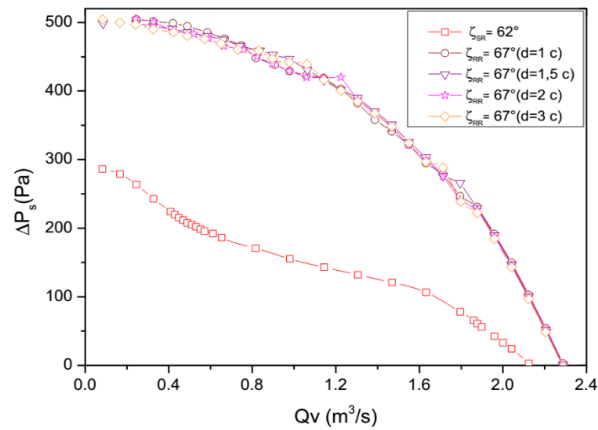

Fig. 19 Static pressure rise of CR case, $\xi_{SR} = 62$ ° $\xi_{RR} = 67$ °

The curve of the static efficiency indicates the best ratio elevation static pressure and power. The total-static efficiency of the counter-rotating fan ($\xi_{FR} = 62$ °) is greater than that of the single-stage fan 62 °, and which reaches its maximum for a flow rate higher than that of the simple fan. The slope of the counter-rotating stage is much higher than that of the single fan. These curves show the interest of the counter-rotating fan when taking the maximum total-static efficiency and which

occupies a higher flow rate range, this yield which does not take into account all the useful energy. For the counter rotating configuration, the nominal flow rate Qv = 1.87 m³/s is very close to the single rotor, but the static pressure rise shows a difference of more than 164 Pa about 95% compared to the case of the single rotor. The total-static efficiency of the counter-rotating system becomes very high, $\eta_{t\text{-}s} \simeq$ 71.2%, whereas it was 64.7% for the single stage, which represents an increase of about 14% compared to the simple rotor SR. The yield curve has a shape similar to that of SR. However, the elevation of the static pressure has a negative slope with strong gradient compared to that of the counter-rotating fan. The difference in total-total efficiency is lower at nominal flow, which is consistent with the work of Shigemitsu and al. [6].
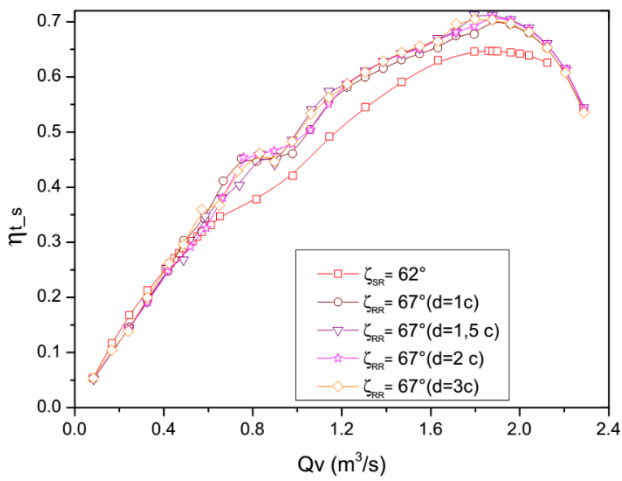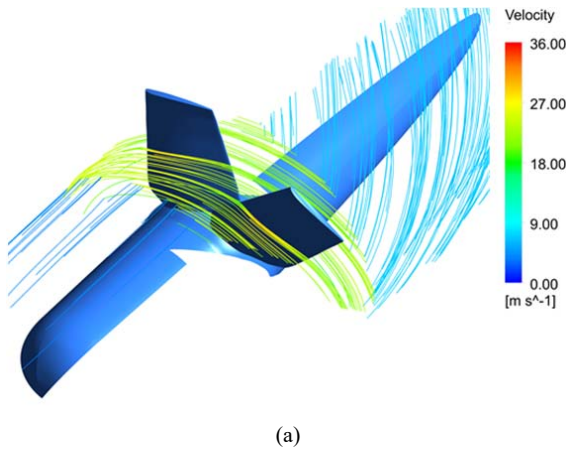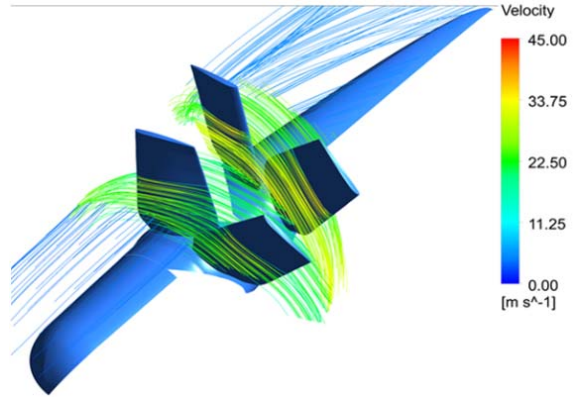

Fig. 20 Efficiency of counter-rotating case CR, ξ_{SR}=62° ξ_{RR} = 67 °

Streamlines

(b)

Fig. 21 Streamlines by the relative velocity a: single rotor (ξ_{SR}=82°, Q_V = 0.61 m³/s b: (ξ_{FR}=82°, ξ_{RR}=84°.Q_V = 0.63m³/s, d=1 c

(a)
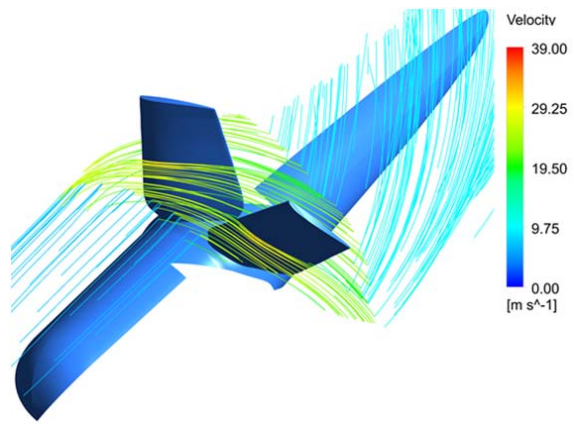
(a)
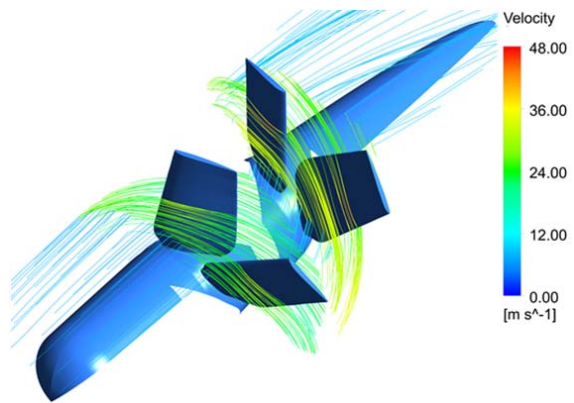
(b)

Fig. 22 Streamlines by the relative velocity a: single rotor (ξ_{SR}=72°, QV = 1.18m³/s b: (ξ_{FR}=72°, ξ_{RR}=76°.Q_V = 1.22m³/s, d=1.5c
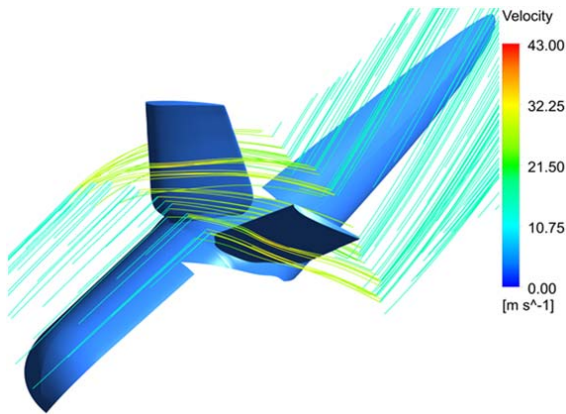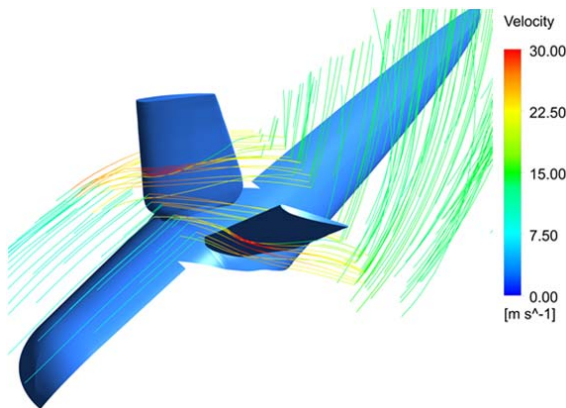
(a)
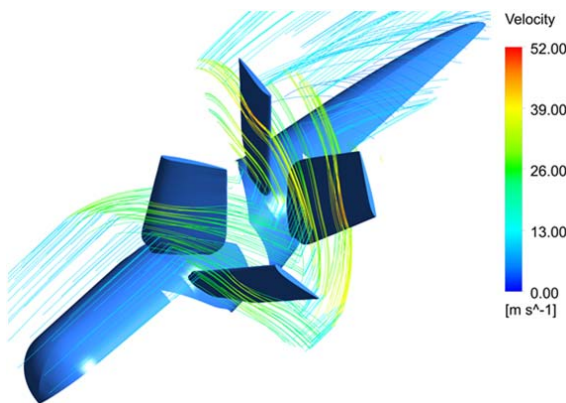
(b)

Fig. 23 Streamlines by the relative velocity a: single rotor (ξ_{SR}=62°,QV = 1.87 m³/s b: (ξ_{FR}=62°, ξ_{RR}=67°.Q_V = 1.87 m³/s, d=1.5c

(a)
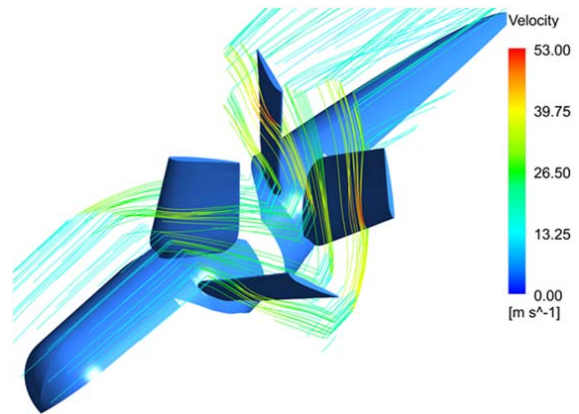
(b)

Fig. 24 Streamlines by the relative velocity a: single rotor (ξ_{SR}=52°, QV = 1.47 m³/s b: (ξ_{FR}=52°, ξ_{RR}=59°.Q_V = 2.53m³/s, d=1.5c

The evolution of the streamlines measured in relative velocity, for 50% of the span and for different blade stagger angles at nominal flow and optimal axial distances. It is clear that the relative velocity at the second counter-rotating rotor is greater than at the first, this is due to the counter-rotating movement which benefits from the gyratory velocity of the flow coming from the first rotor, this gain in relative velocity is translated by a gain in the pressure ratio of the second rotor, this gives interest to reduce the speed of rotation of the rear rotor .

The streamlines recorded in relative velocity show that the outflow of the counter-rotating configuration is axial, which is an objective and considered a significant gain by counter-rotation.

V. CONCLUSION

The counter-rotating rotor systems allow to have more efficient, less noisy machines. As mentioned at the beginning, the main objective of this study is the investigation of performances and the characterization of counter-rotating machines, such as axial fans, and a prediction of the aerodynamic behavior of the flow. The counter-rotating rotor system shows a marked improvement in performance and a significant increase in efficiency compared to the simple rotor case.

The following conclusions can be drawn:
-   The operating ranges are wider and allow for higher efficiency and pressure.
-   The axial distance does not significantly affect the overall performance of the system. It has also been observed that the optimum of the efficiency is obtained for the inter-distance d = 1.5 of cord for all the configurations. This shows that the performance of the contra-rotating system is degraded slightly beyond the limit value of the inter-distance.

REFERENCES

[1]   T. Shigemitsu, J. Fukutomi and Y. Okabe, "Performance and flow

condition of small-sized axial fan and adoption of contra-rotating rotors" Journal of Thermal Science, 2010.

[2] J. Bourne, "A treatise on the screw propeller, with various suggestions of improvement" 2nd Edition, London, 1855.

[3] E. P. Lesley, "Experiments with a counter-propeller" National advisory committee for aeronautics, 1933.

[4] Toru Shigemitsu, Junichiro Fukutomi and Takuya Agawa, "Internal flow condition of high power contra-rotating small- sized axial fan" International Journal of Fluid Machinery and Systems, Vol.6, No.1:25–32, 2013.

[5] Toru Shigemitsu, Junichiro Fukutomi and Hiroki Shimizu,"Influence of blade row distance on performance and flow condition of contra-rotating small-sized axial fan" International Journal of Fluid Machinery and Systems, Vol.5, No.4:161–167, 2012.

[6] T. Shigemitsu, T. Takano, A. Furukawa, K. Okuma and S. Watanabe, "Pressure measurement on casing wall and blade rows interaction of contra-rotating axial flow pump" Journal of Thermal Science, Vol.14, 2005.